$Mn(DBSQ)_2(py)_2$,[21] $Fe(DBSQ)(DBCat)(bpy)$,[45] and $Fe(PhenSQ)(PhenCat)(bpy)\cdot{}^1/_2PhenQ$[45] also show no EPR signal in toluene solution or glass. The reason proposed for this is the strong interaction between the electronic levels on the $S = {}^5/_2$ metals (Mn(II), Fe(III) high spin) and the nearly equivalent levels on the $S = {}^1/_2$ semiquinonate ligands.[45] Thus one plausible explanation for the lack of an EPR signal for **3** is a shift in oxidation state when the compound is in solution to give the all-Mn(II) semiquinonate form $Mn_3(DBSQ)_2(DBCat)_2(py)_4$, in which the Mn(II) ions and the semiquinonate ligands interact to quench the EPR signal. This type of oxidation-state interchange has been previously observed for the systems $Mn^{II}(DBSQ)_2(py)_2/Mn^{IV}(DBCat)_2(py)_2$[21] and $Co^{II}(DBSQ)_2(bpy)/Co^{III}(DBSQ)(DBCat)(bpy)$.[65] In both of these cases the metal centers are in the higher oxidation state in the solid and low-temperature solution and in the lower oxidation state at room temperature in solution. Other closely related compounds are $M^{II}(phth)_2(L)_2$ (M = Mn, L = py;[47] M = Fe, L = $H_2O$[48] (phth = phthiocolato (2-methyl-3-hydroxy-1,4-naphthoquinonato)) which have quinone and phenoxide groups in ortho positions with respect to each other. These compounds do not exhibit this electron-transfer interaction and are always in the lower of the possible metal oxidation states. Thus **3** falls closest to the general category of complexes of the form $M(Q)_2(N\ donor)_2$ (where Q = quinonoid ligand),[21] of which several examples are known where M = Cr → Ni;[65-67] however, **3** is the first example of the stoichiometry $M_3Q_4N_4$.

The UV-visible spectrum of **3** also indicates that oxidation state II prevails for manganese in solution. The dark green-brown crystals of **3** dissolve in toluene to give a light yellow solution similar in appearance to **1** and **2**. Only a single weak absorption is observed below 33 000 $cm^{-1}$ which is characteristic of Mn(II) compounds. The recently reported compound $Mn(PhenSQ)_2(TMEDA)$ had a quite similar spectrum, with one weak absorption in the same region (25 300 vs 26 300 $cm^{-1}$ for **3**).[68]

In summary, the structures of several new manganese and iron catecholate complexes have been described. Furthermore, the utility of the synthetic route involving the reaction of $M[N(SiMe_3)_2]_2$ with catechol for the investigation of metal quinone complex chemistry has been demonstrated. Future work will include more detailed magnetic and redox studies of these compounds as well as the characterization of other oxidation products of manganese and iron catecholates.

**Acknowledgment.** We thank the donors of the Petroleum Research Fund, administered by the American Chemical Society, for financial support. We also thank Professor R. D. Britt and B. E. Sturgeon for experimental assistance.

**Registry No.** **1**, 138982-85-1; **2**, 138982-86-2; **3**, 138956-47-5; **4**, 138956-50-0; **5**, 138982-87-3.

**Supplementary Material Available:** Full tables of structural parameters and refinement data atom coordinates, bond distances and angles, hydrogen coordinates, and anisotropic thermal parameters (59 pages); listings of structure factors (202 pages). Ordering information is given on any current masthead page.

(65) Buchanan, R. M.; Pierpont, C. G. *J. Am. Chem. Soc.* **1980**, *102*, 4951.
(66) Buchanan, R. M.; Clafin, J.; Pierpont, C. G. *Inorg. Chem.* **1983**, *22*, 2552.
(67) Lynch, M. W.; Buchanan, R. M.; Pierpont, C. G.; Hendrickson, D. N. *Inorg. Chem.* **1981**, *20*, 1038.
(68) Döring, M.; Waldbach, T. *Z. Anorg. Allg. Chem.* **1989**, *577*, 93.

Contribution from the Department of Chemical and Biological Sciences, Oregon Graduate Institute of Science and Technology, 19600 N.W. von Neumann Drive, Beaverton, Oregon 97006-1999

# Pathways for Water Oxidation Catalyzed by the $[(bpy)_2Ru(OH_2)]_2O^{4+}$ Ion

James K. Hurst,* Jinzhong Zhou, and Yabin Lei

*Received April 11, 1991*

Resonance Raman (RR) spectra of the ($\mu$-oxo)bis[*cis*-aquabis(2,2'-bipyridine)ruthenium(III)] ion and its congeners in thermodynamically accessible III-IV, IV-V, and V-V higher oxidation states have been obtained in aqueous solutions under a wide range of medium conditions. The RR spectra were dominated by single bands at 370-403 $cm^{-1}$, assignable to the Ru-O-Ru symmetric stretching mode ($\nu_s$) on the basis of their $^{18}O$-isotope induced shifts. From the magnitudes of the shifts, the Ru-O-Ru angles were calculated to be 155-180° for the various oxidation states. A band appearing at 812 $cm^{-1}$ in the V-V ion which shifted to ~780 $cm^{-1}$ in $[^{18}O]H_2O$ was assigned to a Ru=O stretching mode of a terminal oxo ligand. Below pH 0.3 the bridging $\mu$-oxo atom became protonated; for the other ions, hydrogen bonding to the bridge was indicated by $D_2O$-induced solvent shifts in $\nu_s$(Ru-O-Ru). An $^{18}O$-isotope labeling study of the water oxidation reaction established the existence of a pathway in which one atom of $O_2$ was obtained from an aqua ligand. These results combined with published rate data suggest that this pathway involves solvent nucleophilic attack of a terminal oxo atom as the critical oxygen-oxygen bond forming step, with the bridging oxygen atom serving the essential role of activating and/or orienting the reactant $H_2O$ through formation of a strong hydrogen bond. A second major pathway, for which both O atoms were derived from solvent, was also identified, but no definitive evidence was obtained for a pathway for which both O atoms originated in coordinated $H_2O$.

## Introduction

Dimeric ruthenium complexes of the type $(L_2Ru(OH_2))_2O$, where L is 2,2'-bipyridine[1-3] or a ring-substituted analogue,[4,5] display unique catalytic capabilities for water oxidation, both electrochemically and in reactions with strong oxidants in homogeneous solution. These reactions have considerable intrinsic interest, e.g., in understanding how redox metal clusters can overcome kinetic barriers imposed by reactant noncomplementarity and as potential models for biological water oxidation;[5-7] they might also find essential technological roles, e.g., as catalysts for oxidative half-cycles in practical water photolysis systems.[8,9] Nonetheless, their reactivity is presently poorly described, with

* To whom correspondence should be addressed.

(1) Gilbert, J. A.; Eggleston, D. S.; Murphy, W. R., Jr.; Geselowitz, D. A.; Gersten, S. W.; Hodgson, D. W.; Meyer, T. J. *J. Am. Chem. Soc.* **1985**, *107*, 3855.
(2) Honda, K.; Frank, A. J. *J. Chem. Soc., Chem. Commun.* **1984**, 1635.
(3) Collin, J. P.; Sauvage, J. P. *Inorg. Chem.* **1986**, *25*, 135.
(4) Rotzinger, F. P.; Munavalli, S.; Comte, P.; Hurst, J. K.; Gratzel, M.; Pern, F.-J.; Frank, A. J. *J. Am. Chem. Soc.* **1987**, *109*, 6619.
(5) Comte, P.; Nazeeruddin, M. K.; Rotzinger, F. P.; Frank, A. J.; Gratzel, M. *J. Mol. Catal.* **1989**, *52*, 63.
(6) See, e.g.: Weighardt, K. *Angew. Chem., Int. Ed. Engl.* **1989**, *28*, 1153 and references cited therein.
(7) Geselowitz, D.; Meyer, T. J. *Inorg. Chem.* **1990**, *29*, 3894.

0020-1669/92/1331-1010$03.00/0 

major unresolved issues including identification of the oxidation state(s)[10] of the reactive species and their reaction pathways. Mechanisms initially proposed emphasized intramolecular oxidative elimination of $O_2$ from the V–V ion,[1,4] although formation of $HO_2$ and $H_2O_2$ as discrete intermediates or direct formation of $O_2$ by bimolecular reaction of the IV–V ion were also recognized as thermodynamically acceptable alternatives.[1] Implicit in these discussions was the notion that both atoms of the dioxygen product are derived from the *cis*-diaqua ligands. However, subsequent kinetic analyses established that decomposition of the IV–V ion to its III–IV oxidation state was first order,[11] eliminating a bimolecular pathway for this ion and suggesting rate-limiting attack by solvent water to form a peroxy intermediate, which underwent rapid subsequent oxidation to the final products. An isotope-labeling study of the decomposition of the V–V ion was also interpreted as indicating either multiple concurrent pathways involving intramolecular elimination of ruthenyl oxygen atoms and solvent oxidation[12] or a bimolecular pathway involving intermolecular elimination of ruthenyl oxygen atoms.[7] The latter mechanism is inconsistent with the reported first-order rate law for disappearance of the V–V ion, however.[11] An alternative viewpoint, that the IV–IV ion is the catalytically active species, has been advanced for complexes containing 4,4′- and 5,5′-dicarboxyl-substituted bipyridyl ligands.[5,13] This suggestion was based upon measurements indicating that these ions expressed greater electrocatalytic activity than the parent complex ion despite having energetically less accessible higher oxidation states.[4,5] For the 4,4′-carboxy derivative, this suggestion is consistent with the report that the IV–IV ion formed transiently by pulse radiolysis underwent rapid reduction to the III–IV state without intermediary accumulation of more highly oxidized ions.[5]

In this paper, we use resonance Raman (RR) spectroscopy to obtain structural information on the $[Ru(O)(bpy)_2]_2O$ IV–V and V–V ions and to obtain information on ligand substitution rates that is essential to quantitative evaluation of isotopic distribution studies designed to identify the origins of oxygen atoms in the $O_2$ product. The data support the conclusion of Geselowitz and Meyer[7] that at least part of the $O_2$ formed contains oxygen atoms from the ruthenium coordination sites but exclude mechanisms involving intramolecular or intermolecular oxidative elimination of coordinated oxygen atoms.

## Experimental Methods

**Reagents.** The $((bpy)_2Ru(OH)_2)_2O^{4+}$ (III–III) ion was prepared from *cis*-$Ru(bpy)_2Cl_2$ following procedures described in the literature[1] and was isolated as the perchlorate salt. Electronic absorption spectra in 0.5 M $H_2SO_4$ were very similar to published spectra, specifically, $\lambda_{max}$ (log $\epsilon$) 639 (4.30), 283 (4.69), and 243 nm (4.60) for the III–III ion and 446 (4.28), 302 (4.81), and 246 nm (4.76) for the III–IV ion compared to respective literature values[1] of 637 (4.32), 280 (4.70), and 242 nm (4.60) and 444 (4.34), 304 (4.82), and 246 nm (4.77). Additionally, pH-dependent spectral shifts accompanying deprotonation of coordinated aqua ligands in the III–III ions were identical to reported shifts.[1] The isotopically substituted $((bpy)_2Ru(^{18}OH_2))_2{}^{18}O^{4+}$ ions were prepared analogously from *cis*-$Ru(bpy)_2Cl_2$ in 95% $^{18}O$-enriched $H_2O$ (YEDA). Solutions of the $((bpy)_2Ru(O))_2O^{3+}$ (IV–V) and $((bpy)_2Ru(O))_2O^{4+}$ (V–V) ions in 0.1 M phosphate buffer, pH 6, were prepared by constant potential electrolysis at 0.75 and 1.0–1.2 V, respectively, vs a saturated $Na_2SO_4/HgSO_4/Hg$ reference electrode ($E°$ = 0.64 V vs NHE). A three-compartment electrolysis cell was used, which had platinum gauze working and reference electrodes. The cell was immersed in an ice-water bath, and the reference compartment was purged of $H_2$ by bubbling with $N_2$ during the runs. For the IV–V ion, electrolysis was stopped when the current flow ceased; for the V–V ion, the background current remained relatively high, presumably as a consequence of catalytic water oxidation. Electrolysis was therefore terminated when the current had dropped to a constant value. Reagent solutions of $Co^{3+}$ were prepared in the same cell by electrolysis of 0.1 M $Co(ClO_4)_2$ in 1–3 M $HClO_4$ or trifluoromethanesulfonic ($CF_3SO_3H$) acid. The reaction was monitored spectrophotometrically by following the growth of peaks attributable to $Co^{3+}$ at 400 and 606 nm. The $Co^{3+}$ ion concentration was calculated assuming $\epsilon$ = 43 $M^{-1}$ $cm^{-1}$ at 606 nm; this extinction coefficient was evaluated by determining the oxidizing equivalents of the $Co^{3+}$ solutions by adding excess $FeSO_4$ and back-titrating with standardized $KMnO_4$. Typically, solutions containing 50–75 mM $Co^{3+}$ could be prepared in this manner. Although solutions stored at ~10 °C underwent only slow loss of oxidizing titer, all reagent solutions used in these studies were prepared immediately before use. Trifluoromethanesulfonic acid (Minnesota Mining and Manufacturing Corp.) was vacuum distilled; other reagents were best-available grade and used as received. All reagent solutions were prepared from $H_2O$ that had been purified by reverse osmosis/ion-exchange chromatography and then distilled from quartz.

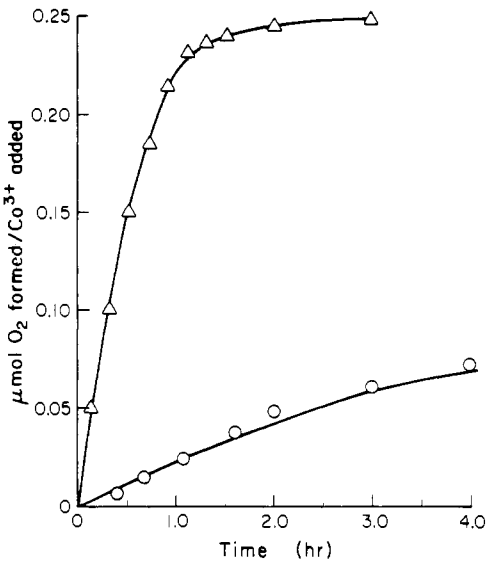


**Figure 1.** $Co^{3+}$ oxidation of $H_2O$. Key: triangles, 0.3 mM $((bpy)_2Ru(OH_2))_2O^{4+}$, 2 mM $Co^{3+}$, in 0.5 M $H_2SO_4$ at 23 °C; circles, identical conditions, except that the ruthenium μ-oxo ion was omitted. The $O_2$ yield corresponds to a catalyst turnover number of 15.

**Methods.** Oxygen evolution was monitored using a YSI Type 4004 polarographic electrode poised at 0.6 V vs its internal Ag/AgCl reference electrode. The electrode was mounted to sample headspace gases in a thermostated reaction cell that could accept reactants and purging gases through septum-fitted openings. The electrode response was recorded by connecting it to a strip chart; the system was calibrated by injecting known amounts of air into the reaction cell and measuring the resulting pen displacement.

Isotopic ratios of $O_2$ produced by water oxidation were determined using a Finnigan 4000 gas chromatography/EI-CI mass spectrometer system operated in the electron impact mode at 70 eV. The spectra were repetitively scanned every 0.5 s over a mass range of 15–200 amu during the period that the samples were introduced. Current maxima for each of the ions appeared at the same temporal position, and their intensity decay profiles were identical. Oxygen isotope ratios were determined from the mass spectra corresponding to the maximal ion currents. The apparatus for initiating the reaction and isolating gaseous products has been previously described.[14] Briefly, reactants isolated in the main chamber and side arm of an evacuable reaction cell were subjected to several freeze–pump–thaw cycles to remove dissolved gases, and then reactants were mixed in vacuo and gases evolved were isolated by con-

(8) *Energy Resources Through Photochemistry and Catalysis*; Gratzel, M., Ed.; Academic Press: New York, 1983.
(9) *Photochemical Conversion and Storage of Solar Energy*; Connolly, J. S., Ed.; Academic Press: New York, 1981.
(10) For the (μ-oxo)bis[*cis*-aquabis(2,2′-bipyridine)ruthenium] ion, four oxidation states have been detected in aqueous solution and assigned from electrochemical studies to ruthenium in its III–III, III–IV, IV–V, and V–V formal oxidation states.[1] Metal ion oxidation was accompanied by progressive deprotonation of coordinated $H_2O$, ultimately giving terminal oxo atoms in the IV–V and V–V ions. For analogous complexes containing carboxyl-substituted bipyridines, only the III–III and III–IV ions were thermodynamically accessible in aqueous solution.[4,5] For all ions, reduction below the III–III state gave hydrolytic cleavage of the oxo bridge at rates that were dependent upon the identity of the bipyridyl ligand.
(11) Raven, S. J.; Meyer, T. J. *Inorg. Chem.* **1988**, *27*, 4478.
(12) Meyer, T. J. In *Oxygen Complexes and Oxygen Activation by Transition Metals*; Martell, A. E., Sawyer, D. T., Eds.; Plenum Press: New York, 1988; pp 33–48.
(13) Nazeeruddin, M. K.; Rotzinger, F. P.; Comte, P.; Gratzel, M. *J. Chem. Soc., Chem. Commun.* **1988**, 872.
(14) Zhou, J.; Xi, W.; Hurst, J. K. *Inorg. Chem.* **1990**, *29*, 160.

**Table I.** Origins of O Atoms in $O_2$ from Dimer-Catalyzed $H_2O$ Oxidation[a]

| $[Ru_2O]$, mM | [Oxidant]/$[Ru_2O]$ | collcn interval,[b] min | % distribution: both O from $H_2O$ | one O from $Ru_2O$ | both O from $Ru_2O$ |
|---|---|---|---|---|---|
| | | A. This Work | | | |
| 1.0[c] | 5.8 | 0–30 | 58 | 42 | 0 |
| 1.1 | 5.5 | 0–30 | 35 | 56 | 9 |
| 1.2 | 6.7 | 0–5 | 39 | 58 | 3 |
| | | 5–15 | 51 | 46 | 3 |
| | | 5–30 | 56 | 40 | 4 |
| | | 30–60 | 77 | 21 | 2 |
| 9.9 | 6.3 | 0–2 | 61 | 41 | −2 |
| | | 2–4.5 | 65 | 37 | −2 |
| | | 4.5–7 | 66 | 36 | −2 |
| | | 7–10 | 66 | 36 | −2 |
| | | 10–13 | 66 | 36 | −2 |
| | | 13–16 | 66 | 36 | −2 |
| | | 16–20 | 66 | 35 | −1 |
| 1.5 | 4.6 | 4–8 | 57 | 42 | 1 |
| | | B. Calculated from Ref 7[d] | | | |
| 1.0 | 5.0 | 0–60 | 21 | 69 | 10 |

[a] $Co^{3+}$ oxidant, at ambient temperature, in 1 M $CF_3SO_3H$ except where indicated. [b] 0 time is the point of initiation of reaction. [c] In 1 M $HClO_4$. [d] $Ce^{4+}$ oxidant, in 0.1 M $CF_3SO_3H$.

densation in a small tube attached to the vacuum line that was cooled in liquid $N_2$. For studies involving temporal changes in $O_2$ isotopic distributions, the collection tube was modified to permit simultaneous attachment to the vacuum manifold of the reaction chamber and the mass spectrometer. This arrangement allowed repetitive sampling of evolved gases with time intervals as short as 2 min. Background experiments in which oxidant and/or catalyst were omitted established that the apparatus was airtight over the entire reaction time period.

Resonance Raman (RR) spectra were recorded on a computer-controlled Jarrel-Ash instrument[15] with excitation from either Spectra Physics Model 164 argon ion or Spectra Physics Model 2025 krypton ion lasers. Sample preparation and analyses were identical to previously reported methods for other dimeric ($\mu$-oxo)ruthenium ions.[14]

## Results and Discussion

**Reaction Stoichiometry.** Oxygen evolution began immediately upon adding $Co^{3+}$ to acidic solutions containing micromolar concentrations of the $((bpy)_2Ru(OH_2))_2O^{4+}$ ion; the reaction proceeded vigorously until the $Co^{3+}$ ion was consumed. A typical result is given in Figure 1; for comparison, the rate of oxygen evolution when the ruthenium $\mu$-oxo ion was absent is also given. Greater than 95% of the initial added ruthenium complex remained upon completion of the reaction, indicating that degradative side reactions were negligible. (The ion present in product solutions was the one-electron-oxidized III–IV dimer, which is stable under the experimental conditions.)[1] In the present example, the amount of $O_2$ formed corresponded to a turnover number of 15 for the dimer, based upon a four-electron cycle. The oxygen yield (Figure 1) was very nearly the stoichiometric amount expected for the reaction:

$$4Co^{3+} + 2H_2O \rightarrow 4Co^{2+} + 4H^+ + O_2$$

These combined results indicate that the ruthenium dimer is a true catalyst for the reaction. Identical results were obtained for reactions carried out in 0.5 M $H_2SO_4$, 1.0 M $HClO_4$, and 1.0 M $CF_3SO_3H$.

**Isotope Labeling Studies.** Apart from the qualitative observation that the III–III ion is considerably more labile than the III–IV ion,[7] rates of aqua exchange on the catalyst have not been reported. Comparisons of $O_2$ isotopic distributions using varying protocols indicate that exchange of coordinated $H_2O$ with bulk solvent was surprisingly rapid in the III–III ion. For example, when perchlorate salts of the $^{18}O$-labeled III–III ion were dissolved in 0.5 M $H_2SO_4$ of normal isotopic composition, then immediately outgassed by evacuation, and $Co^{3+}$ added, the isotopic distribution of dioxygen recovered was >90% $^{32}O_2$, ~9% $^{34}O_2$, and <1% $^{36}O_2$; similar experiments using a complex ion with normal isotopic distribution in 85% $^{18}O$-enriched $H_2O$ gave <1% $^{32}O_2$, 27% $^{34}O_2$, and 73% $^{36}O_2$. However, when the $^{18}O$-labeled III–III ion was dissolved in $^{18}O$-enriched $H_2O$ and outgassed before isotopic dilution with normal solvent containing the oxidant, a much larger percentage composition of $^{34}O_2$ was measured (Table I). Since other reaction conditions were nearly identical, the basis for the differing results must reside in isotopic scrambling of the coordinated $^{18}O$ by exchange with solvent during the degassing procedure. Since this required less than 30 min, during most of which time the solution was cold or frozen, the results suggest that $t_{1/2} < 15$ min for aqua exchange under ambient conditions. This can be compared to mononuclear complexes, for which substitution on Ru(III) by dissociative pathways is very slow ($t_{1/2} \simeq$ several hours);[16] the crystal structure of the $((bpy)_2Ru(OH_2))_2O^{4+}$ ion contains no features that would suggest promotion of water exchange by associative pathways.[1,16]

To prevent loss of isotopic label prior to reaction with oxidant, the $^{18}O$-substituted III–III ion was dissolved and the solution incubated in $^{18}O$-enriched $H_2O$ for 5–10 min at 60 °C before introduction into the reaction chamber. Typically, 5–26 mg of the perchlorate salts were dissolved in 0.2–0.3 mL of 97% $[^{18}O]H_2O$, degassed, and then reacted with sufficient $Co^{3+}$ reagent in 2.6 mL of 1 M $CF_3SO_3H$ or $HClO_4$ to give a $Co^{3+}$/dimer ratio of 5–6. Product gases were always analyzed within 30 min after initiating the reaction, a point at which water oxidation was ~50% complete (Figure 1). Experimental conditions therefore corresponded to less than a single turnover for the catalytic ions. Results are summarized in Table I, where the percentage yields of $O_2$ formed containing both oxygen atoms derived from solvent and for one and two O atoms derived from the coordination complex have been calculted from the measured $O_2$ isotopic distributions and the known distributions of the complex and solvent at the start of the reaction. The data have been corrected for background atmospheric $^{32}O_2$ by subtracting 20% of the counts measured for $m/z = 28$ ($N_2$) from the total counts at $m/z = 32$. Usually this correction was minor, comprising <5% of the total counts, but for a few samples air leakage gave background levels that were as high as 58% of the total counts. Even in these extreme instances, the corrected relative isotopic yields were comparable to results for uncontaminated samples. In 1 M $HClO_4$, the catalyst precipitated when oxidized; this precipitate persisted for the duration of the reaction and then redissolved to give the spectrally identified III–IV ion. Despite this complication, results were comparable to those obtained in 1 M $CF_3SO_3H$, where precipitation did not occur (Table I).

For all runs, roughly half of the $O_2$ formed acquired both oxygen atoms from solvent, with the remainder acquiring one oxygen from the complex and one oxygen from the solvent. These results are similar to those reported earlier[7] (Table I), with the exception that our data provide no clear evidence for $O_2$ formation by a mechanism in which both oxygen atoms are derived from the coordination complex. Quantitative differences in the two studies might be attributable to differing reaction conditions, specifically the oxidant used ($Co^{3+}$ vs $Ce^{4+}$) and the medium acidity (pH 0 vs pH 1). One important question not answered by the earlier study was the extent to which aqua exchange in the catalytic ions in their higher oxidation states might lead to isotopic scrambling. If this occurred over the time course of the water oxidation reaction, then assignment of the various $O_2$ isotopic products to specific reaction pathways could not be made; i.e., formation of $^{32}O_2$ and $^{34}O_2$ might be due to progressive accumulation of $^{16}O$ in the complex by aqua exchange with coordinated $^{18}O$-containing $H_2O$. Our data examining incremental changes over the reaction course (Table I, third and fourth data sets) show isotopic distributions that are nearly constant with time. The small changes observed are consistent with isotopic dilution arising from replacement of $^{18}O$ atoms incorporated from the complex into $O_2$

(15) Loehr, T. M.; Keyes, W. E.; Pincus, P. A. *Anal. Biochem.* **1979**, *96*, 456.

(16) See, e.g.: Matsubara, T.; Creutz, C. *Inorg. Chem.* **1979**, *18*, 1956.

**Table II.** μ-Oxo Ion Resonance Raman Band Assignments and Positions

| ion | $\nu_s$(M–O–M),[a] cm$^{-1}$ | $\Delta\nu$($^{16}$O–$^{18}$O),[b] cm$^{-1}$ | $\Delta\nu$($H_2O$–$D_2O$), cm$^{-1}$ | other modes, cm$^{-1}$ |
|---|---|---|---|---|
| | | A. III–III | | |
| $((bpy)_2Ru(OH_2))_2O^{4+}$ | ~370 (741) | 2 (3) | 2 (3) | $\nu_{as}$(M–O–M): 824 (790)[c] |
| $(bpy)_2Ru(OH)ORu(OH_2)(bpy)_2^{3+}$ | ~370 (750) | 3 (6) | 3 (5) | |
| $((bpy)_2Ru(OH))_2O^{2+}$ | 378 (763) | n.d. | n.d. | |
| | | B. III–IV | | |
| $((bpy)_2Ru(OH_2))_2O^{5+}$ | 402 (797) | 8–9 (15) | 1 | |
| $(bpy)_2Ru(OH)ORu(OH_2)(bpy)_2^{4+}$ | 395 (786) | 5 | ~0 | |
| $((bpy)_2Ru(OH))_2O^{3+}$ | 392 | n.d. | 5 | |
| | | C. IV–V | | |
| $((bpy)_2Ru(O))_2O^{3+}$ | 394 (770)[d] | 7 | n.d. | |
| | | D. V–V | | |
| $((bpy)_2Ru(O))_2O^{4+}$ | 370 (744)[d] | 8 | n.d. | ν(Ru=O): 812 |
| $((bpy)_2Ru(O))_2OH^{5+}$ | 360 (730) | 0–1 | n.d. | ν(Ru=O): 816 |

[a] Values in parentheses are approximate maxima measured for $2\nu_s$. [b] Values in parentheses are shifts in $2\nu_s$. [c] Values in parentheses are $\nu_{as}$ values for the $^{18}$O-substituted ion. [d] Measured at pH 1.

by $^{16}$O-containing water. These observations allow two conclusions to be drawn: (1) aqua exchange was insignificant on the reaction time scale for the dimer in its higher oxidation states and, consequently, (2) the $^{32}O_2$ and $^{34}O_2$ were formed by different reaction pathways.

**Resonance Raman Spectra. General Observations.** In $C_{2v}$ symmetry, i.e., when the bridge is bent, the three-body system M–O–M has three normal coordinate motions comprising symmetric ($\nu_s$) and asymmetric ($\nu_{as}$) stretching modes and a bending ($\delta$) mode. All three modes are Raman-active, but $\nu_s$ is expected to be much more intense than the others. The $\nu_s$ and $\nu_{as}$ frequencies depend strongly upon the M–O–M angle but should lie in the regions $\nu_s$ = 300–500 cm$^{-1}$ and $\nu_{as}$ = 750–950 cm$^{-1}$ when the bridge is nearly linear.[17] These theoretical expectations have been confirmed for a variety of μ-oxo-bridged systems.[18] In these cases, $\delta$(M–O–M) is calculated to lie below 200 cm$^{-1}$, but a band that is sensitive to isotopic substitution in the bridging atom has occasionally been observed at about 300 cm$^{-1}$. This behavior has been interpreted to indicate that the $\delta$(M–O–M) mode is coupled to the stretching motions of other ligand atoms.

The RR spectra of each of the μ-oxo ions examined in this study were dominated by single strong bands in the region 360–405 cm$^{-1}$ which shifted slightly to lower energies upon $^{18}$O substitution in the bridge. On the basis of these properties, these bands can be assigned to the $\nu_s$(M–O–M) modes. They were always accompanied by broad, weaker bands at twice the energy, which are undoubtedly their first overtones, i.e., $2\nu_s$(M–O–M). Band maxima and other spectral properties of the individual ions are described in the following sections; spectral assignments and band positions are compiled in Table II.

**The $((bpy)_2Ru(OH_2))_2O^{4+}$ (III–III) Ion.** The position maximum of $\nu_s$(M–O–M) for this ion was difficult to determine accurately because two maxima appeared in the region of strong absorption (Figure 2). Nonetheless, it was evident from the character of $^{18}$O-isotope or $D_2O$ solvent-induced shifts that the peak intensity was dominated by a single band, i.e., the difference spectra gave simple, symmetrical band shapes (Figure 2C). Deprotonation constants for the aqua ligands are p$K_{a1}$ = 5.9 and p$K_{a2}$ = 8.3.[1] With the exception that the weak 329-cm$^{-1}$ band (Figure 2) was lost above pH 6, RR spectra of the complex ion over the range pH 0–8 were nearly identical. Above pH 10, in 0.1 M phosphate buffer, $\nu_s$(M–O–M) underwent an ~10-cm$^{-1}$ shift to higher energies and numerous changes occurred in minor bands in the region 280–500 cm$^{-1}$, suggesting that a relatively large structural change may have occurred. In acidic to neutral $D_2O$ solutions, the bands at 370 cm$^{-1}$ ($\nu_s$) and 740 cm$^{-1}$ ($2\nu_s$) underwent shifts of 2–4 cm$^{-1}$ to lower energies; in acidic media, a small bathochromic shift ($\Delta\nu$ = 2 cm$^{-1}$) was also observed for the 329-cm$^{-1}$ band. Positions and intensities of all other bands were unchanged. Effects of this magnitude have previously been measured for ferric μ-oxo ions and attributed to strong hydrogen bonding of the bridging oxo atom.[19] The $\nu_s$ and $2\nu_s$ bands in the

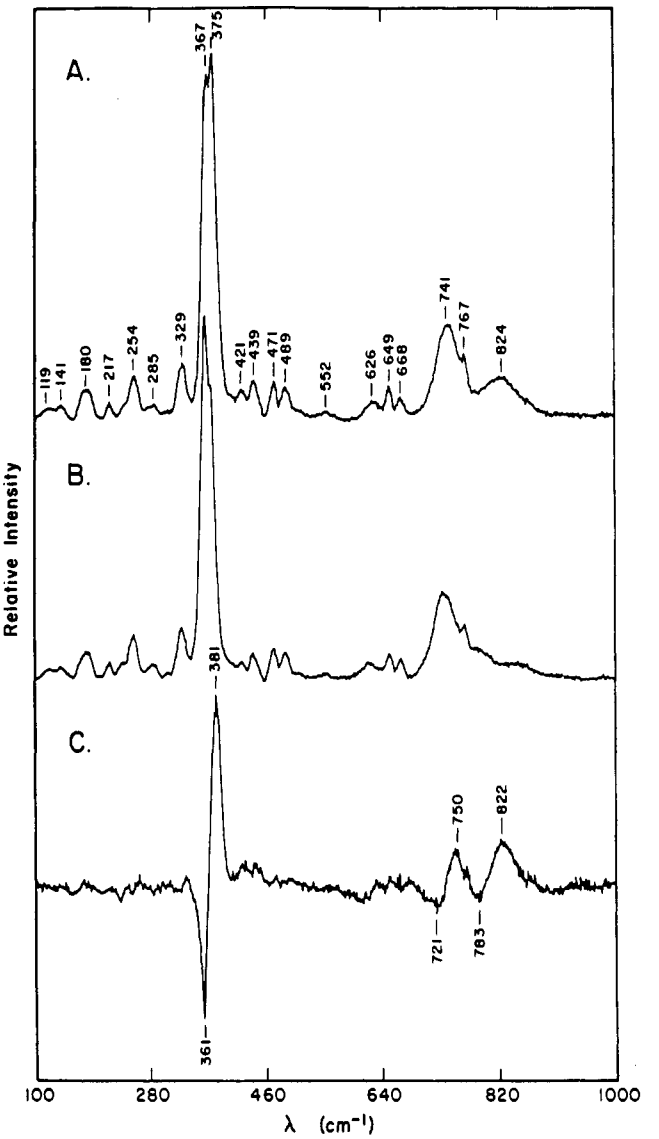


**Figure 2.** Resonance Raman spectra of the $((bpy)_2Ru(OH_2))_2O^{4+}$ (III–III) ion. Key: (A) normal isotope; (B) $^{18}$O-enriched; (C) A – B difference spectrum. Conditions: 1–2 mM complex ion in 0.1 M $HClO_4$, $T$ = 90 K; 60-mW excitation at 647 nm. Spectra are averages of 12 scans taken at 8-cm$^{-1}$ slit width and 1 cm$^{-1}$/s scan rate; the background was subtracted, but no smoothing routines were applied.

(17) Wing, R. M.; Callahan, K. P. *Inorg. Chem.* **1969**, *8*, 871.
(18) Loehr, T. M.; Shiemke, A. K. In *Biological Applications of Raman Spectroscopy*; Spiro, T. G., Ed.; Wiley: New York, 1988; Vol. 3, Chapter 10.

isotopically substituted ion, $((bpy)_2Ru(^{18}OH_2))_2{}^{18}O^{4+}$, were also shifted by 3–6 $cm^{-1}$ to lower energies relative to the parent compound, but the 329-$cm^{-1}$ band position did not change. The broad band at 824 $cm^{-1}$ in the normal isotope spectrum disappeared and a high-energy shoulder appeared on the broad 740-$cm^{-1}$ band (Figure 2), suggesting that the band had shifted by $\Delta\nu \simeq 40$ $cm^{-1}$. No other spectral changes were observed. The ligand and solvent isotopic effects appeared to be additive.

The RR spectra of liquid samples taken with 90° scattering using a Dilor 724 instrument and of the solid perchlorate salts diluted in KBr[14] were essentially identical to the frozen solution spectra; other than the appearance of weak bands attributable to the normal Raman spectra of the oxyanions, spectra taken in perchlorate-, phosphate-, and sulfate-containing media were identical. No photodecomposition of the samples in the laser beam was noticed, and exposure of the $((bpy)_2Ru(OH_2))_2O^{4+}$ ion in 0.5 M $H_2SO_4$ to an intense visible light beam ($\lambda > 350$ nm) for 90 min caused no change in the RR spectrum of the ion.

The large shift in the weak 824-$cm^{-1}$ band upon $^{18}O$-isotopic substitution is consistent with its assignment as the $\nu_{as}$(M–O–M) stretching mode. Confirmation was sought by examining the FTIR spectra of the perchlorate salts in KBr. However, no bands were observed in the region between 800 and 1000 $cm^{-1}$ and strong bipyridine ligand bands obscured the region immediately below 800 $cm^{-1}$. $^{18}O$-induced isotope shifts were not observed for any vibrational bands in the FTIR spectra. The small shift in the RR spectrum observed at 329 $cm^{-1}$ in $D_2O$ might indicate that it contains as a component the $\delta$(M–O–M) bending motion, although this assignment is tenuous since no comparable shift was observed for the $^{18}O$-substituted ion. The shift is too small for the metal–aqua stretching motion ($\Delta\nu \simeq 19$ $cm^{-1}$ for a pure Ru–$OH_2$ mode) and, on the basis of the absence of detectable shifts in either $D_2O$ or upon $^{18}O$-substitution, none of the other bands appearing in the 200–500-$cm^{-1}$ region can be assigned to this motion.

**The $((bpy)_2Ru(OH_2))_2O^{5+}$ (III–IV) Ion.** The dominant feature of the RR spectrum for this ion was a single band at 402 $cm^{-1}$, which shifted to 393 $cm^{-1}$ upon $^{18}O$-substitution (Figure 3). On the basis of these properties, it can be assigned to the $\nu_s$(M–O–M) mode. This band is relatively less intense than for the III–III ions; correspondingly, the $2\nu_s$ overtone and $\nu_{as}$ modes were not well defined. Two deprotonation constants have been determined[1] for the III–IV ion, for which $pK_{a1} = 0.4$ and $pK_{a2} = 3.3$. Sequential loss of one and two protons from coordinated $H_2O$ caused $\nu_s$ to shift progressively to lower energies, with band maxima appearing at 395 and 392 $cm^{-1}$, respectively, at pH 2 and 6. The spectrum of the diaqua complex was insensitive to solvent isotopic composition, exhibiting only barely detectable shifts to lower energy of the 402- and 350-$cm^{-1}$ bands in $D_2O$ and no perturbation in $H_2{}^{18}O$. The hydroxo–aqua ion was similarly solvent-insensitive, but the dihydroxo ion exhibited relatively large $D_2O$-induced ($\Delta\nu$ = 3–5 $cm^{-1}$) shifts to lower energy in both its 353- and 392-$cm^{-1}$ bands. No other shifts, either solvent-induced or from $^{18}O$-isotopic substitution, were observed in the RR spectra of the ions. In particular, no bands assignable to the Ru–O stretching frequencies of the coordinated aqua ligands could be found. Except for normal Raman bands attributable to the counterions, spectra of the III–IV ions were identical in aqueous $HClO_4$ and $H_2SO_4$ media. No photodecomposition was detected for the III–IV ions in frozen solution, but the room-temperature spectrum of the hydroxo–aqua ion in 0.1 M $HClO_4$ gave an asymmetric $\nu_s$ band with a maximum at 390 $cm^{-1}$, rather than 395 $cm^{-1}$, suggesting possible laser-induced degradation under these conditions.

Oxygen exchange in the Ru–O–Ru bridge was briefly examined by following temporal changes in the $\nu_s$ band position. No spectral changes were observed when the $^{18}O$-complex (or $^{16}O$-complex) was incubated in $H_2{}^{16}O$ (or $H_2{}^{18}O$), pH 0 ($HClO_4$ or $H_2SO_4$), at room temperature for periods up to 30 h. Small shifts consistent with partial isotopic exchange in the bridge were detected after heating the samples to 60 °C for 5 h; exchange appeared complete

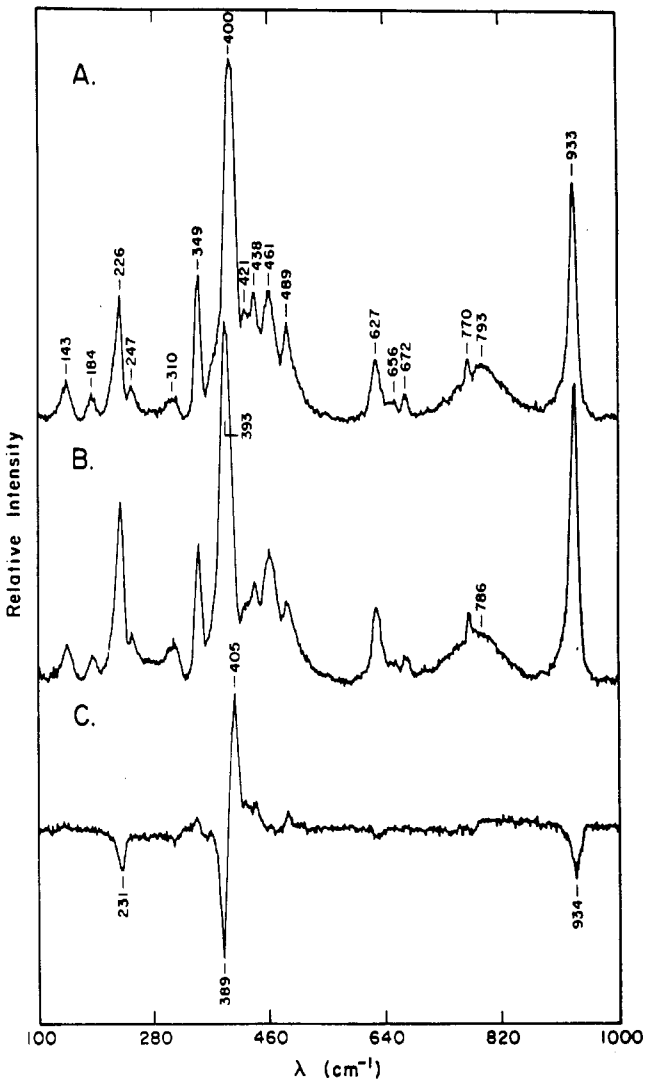


**Figure 3.** Resonance Raman spectra of the $((bpy)_2Ru(OH_2)_2O^{5+}$ ion. Key: (A) normal isotope; (B) $^{18}O$-enriched; (C) A – B difference spectrum. Conditions are the same as in Figure 2 except the following: 1 M $HClO_4$; 50-mW excitation at 514 nm; 16 scans averaged. The minima in spectrum C at 231 and 934 $cm^{-1}$ are attributable to solvent and perchlorate modes, respectively.

by 47 h at this temperature or upon heating to 80 °C for about 8 h. In 1 M $HClO_4$, heating to 90 °C caused loss of peak symmetry and the appearance of new, medium-intensity isotope-sensitive bands in the region 770–810 $cm^{-1}$, suggesting structural modification or complex decomposition.

RR spectra of product solutions used in isotopic labeling studies of $((bpy)_2Ru(OH_2))_2O$-catalyzed water oxidation by $Co^{3+}$ indicated that isotopic substitution at the bridging oxo had not occurred during turnover; i.e., the $\nu_s$ position was identical before and immediately following the reaction.

**Higher Oxidation States. a. $\nu_s$ Mode.** Incremental addition of $Co^{3+}$ to solutions containing the $(bpy)_2(Ru(OH)ORu(OH_2)(bpy)_2{}^{4+}$ ion in 0.1 M $HClO_4$ or $CF_3SO_3H$ caused progressive loss in intensity of the $\nu_s$ band of the III–IV ion with appearance of a new band at 394 $cm^{-1}$, which then also decreased in intensity in favor of a third band at 370 $cm^{-1}$ when the oxidative titration was continued (Figure 4). Analogous behavior was observed for the $^{18}O$-substituted ion, with the corresponding band positions being 387 $cm^{-1}$ for the intermediate oxidation state and 362 $cm^{-1}$ for the most highly oxidized complex ion. In 1 M $HClO_4$ or $CF_3SO_3H$, $Co^{3+}$ oxidation of the $((bpy)_2Ru(OH_2))_2O^{5+}$ ion gave only a single species whose RR spectrum was distinguished by a major band at 360 $cm^{-1}$ and a new, medium-intensity band at 816 $cm^{-1}$. Constant-potential electrolysis in 0.1 M phosphate, pH 6, at 0.75 V vs saturated $Na_2SO_4/HgSO_4/Hg$ gave an ion

(19) Shiemke, A. D.; Loehr, T. M.; Sanders-Loehr, J. *J. Am. Chem. Soc.* **1986**, *108*, 2437.

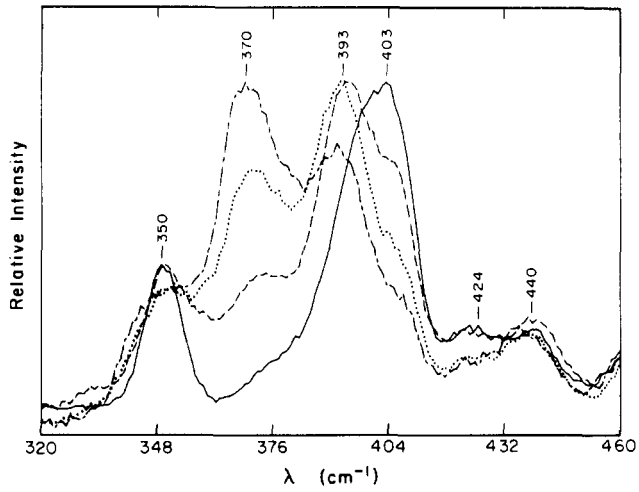


**Figure 4.** Resonance Raman spectra of the $Co^{3+}$ titration of the $(bpy)_2Ru(OH)ORu(OH_2)(bpy)_2^{4+}$ (III–IV) ion. Key: solid line, reference spectrum, obtained by $Ce^{4+}$ oxidation of 2 mM $((bpy)_2Ru(OH_2))_2O^{4+}$; dashed line, +1.5 equiv of 33 mM $Co^{3+}$; dotted line, +2.2 equiv of $Co^{3+}$; dot-dashed line, +5.3 equiv of $Co^{3+}$. Conditions are the same as in Figure 3, except for 0.1 M $CF_3SO_3H$ and six scans averaged.

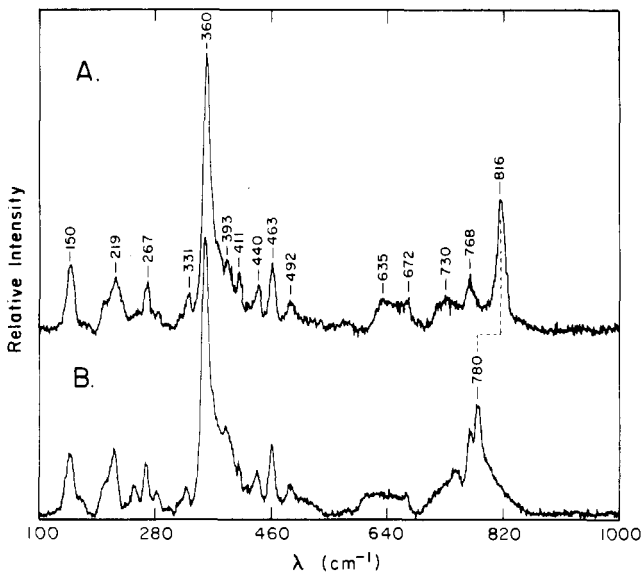


**Figure 5.** Solvent dependence of the $((bpy)_2Ru(O))_2OH^{3+}$ (V–V) resonance Raman spectrum. Key: (A) $Co^{3+}$-oxidized $^{18}O$-substituted $((bpy)_2Ru(OH_2))_2O^{4+}$ ion in normal $H_2O$; (B) same ion in 80% $^{18}O$-enriched $H_2O$. Conditions are the same as in Figure 3, except for 1 M $CF_3SO_3H$ and three scans averaged.

whose RR spectrum closely resembled the intermediate formed by $Co^{3+}$ titration in weakly acidic media, except that the major peak was shifted to 385 $cm^{-1}$; electrolysis at 1.2 V gave extensive conversion to a species whose RR spectrum was nearly identical to the most highly $Co^{3+}$-oxidized ion, with a major peak at 367 $cm^{-1}$.

The reactivity of the ruthenium μ-oxo dimers in their higher oxidation states has been examined using electrochemical methods. Thermodynamically stable states that have been identified in neutral to weakly acidic solutions include the IV–V and V–V ions; in strong acid, the IV–V ion was unstable to disproportionation to the V–V and III–IV states.[1] The reactivity patterns revealed by RR spectroscopy are consistent with this analysis; accordingly, the species with $\nu_s$ = 394 $cm^{-1}$ in 0.1 M acidic media is identified as the IV–V ion and the species with $\nu_s$ = 370 $cm^{-1}$ as the V–V ion. The pH dependence of electrochemical potentials for these ions has been interpreted to indicate that they are both ruthenyl ions,[1] i.e., $((bpy)Ru(O))_2O^{3+/4+}$. This leaves unaccounted the basis for the 370- to 360-$cm^{-1}$ shift observed for the V–V ion in strong acid. The direction of the shift and absence of perturbation of other vibrational modes suggests that it is due to protonation of the bridging μ-oxo atom. Similar protonation in strongly acidic media has been inferred from the rate law for $O_2$-evolving decomposition of a dimeric manganese(IV) ion containing a single μ-peroxo and two μ-oxo bridging ligands; the kinetically determined protonation constant, presumably involving a μ-oxo site, was $pK_a \simeq 1$.[20] Protonation of a bridging μ-oxo atom within a $Mn_4O_6^{4+}$ tetranuclear complex has also been reported, for which $pK_a \simeq 3.5$.[21] In 0.2–0.3 M $CF_3SO_3H$, both 360- and 370-$cm^{-1}$ bands were observed in the V–V ion RR spectra, consistent with the simultaneous presence of the hydroxo- and oxo-bridged forms. On the basis of this observation, the protonation constant for the reaction

$$H^+ + ((bpy)_2Ru(O))_2O^{4+} \rightleftharpoons ((bpy)_2Ru(O))_2OH^{3+}$$

is $pK_a \simeq 0.6$.

**b. Other RR Modes.** Other features of the RR spectra were very similar to the III–IV ion, with the exception that a new pH-sensitive band of medium intensity appeared in the spectrum of the V–V ion. When the normal isotope was oxidized in normal solvent, the band appeared at 812 $cm^{-1}$ (pH 1) or 816 $cm^{-1}$ (pH 0); corresponding bands for the $^{18}O$-substituted complex were 807 $cm^{-1}$ (pH 1) and 816 $cm^{-1}$ (pH 0). In ~80% $[^{18}O]H_2O$, 1 M $CF_3SO_3H$, the bands were at ~767 $cm^{-1}$ for the normal isotope and ~780 $cm^{-1}$ for the $^{18}O$-substituted complex ion. For these experiments, the III–III perchlorate salts were incubated 15–30 min before oxidation with $Co^{3+}$. On the basis of the previously described $O_2$ isotopic distribution and RR spectral data, this time interval is sufficient to equilibrate the cis-aqua ligands and solvent but will give negligible isotopic substitution in the bridging oxo position. The large solvent isotope effects ($\Delta\nu$ = 36–49 $cm^{-1}$) and minor bridging atom isotope effects ($\Delta\nu$ = 0–5 $cm^{-1}$) observed therefore implicate vibrational motions involving the terminal oxo atoms as the source of this band. Consistent with this behavior, the band also appeared at 803 $cm^{-1}$ in the RR spectrum of the electrolytically prepared V–V ion in 0.1 M phosphate, pH 6.

The V–V ions underwent fairly rapid photoreduction in frozen solution (at 90 K) in the laser beam. The product ion at pH 1–6 was the IV–V ion, which appeared stable under these conditions; at pH 0, however, the observable product was the III–IV ion. This photosensitivity caused difficulties in obtaining a pure RR spectrum of the V–V ion. A second problem encountered in perchlorate-containing solutions was precipitation of the IV–V and V–V ions. The spectra of all samples reverted to that of the III–IV ion after several hours' storage of the samples at room temperature; during this time, gas bubbles formed in the capillary tubes.

**c. Assignment of the 812-$cm^{-1}$ RR Band.** The band is in a frequency range where $\nu_{as}$(Ru–O–Ru), $\nu$(O–O) peroxo stretching,[22] or $\nu$(Ru=O) ruthenyl stretching modes[23–25] are expected to appear. Of these possibilities, the first can be eliminated because it cannot account for the large solvent-dependent shift to lower energies ($\Delta\nu \simeq -40$ $cm^{-1}$) observed when the complexes were dissolved in $^{18}O$-enriched $H_2O$ under conditions where isotopic substitution had not occurred in the bridging atom. In the absence of additional information, the other two modes are equally plausible. The magnitude of the solvent-induced isotope shift is very nearly that expected for $^{18}O$ substitution for pure M=O ($\Delta\nu$ = 40 $cm^{-1}$) or peroxo ($\Delta\nu$ = 47 $cm^{-1}$) stretching modes. Both peroxo-bridged species[1,4] and monodentate peroxo-ligand complexes[12] have been proposed as intermediates in the catalytic cycle for water oxidation. However, spatial constraints imposed by the nearly linear Ru–

(20) Wieghardt, K. Personal communication.
(21) Hagen, K. S.; Westmoreland, T. D.; Scott, M. J.; Armstrong, W. H. *J. Am. Chem. Soc.* **1989**, *111*, 1907.
(22) See, e.g.: Nakamoto, K. *Infrared and Raman Spectra of Inorganic and Coordination Compounds*, 4th ed.; Wiley: New York, 1986.
(23) Lincoln, S. E.; Loehr, T. M. *Inorg. Chem.* **1990**, *29*, 1907.
(24) Terner, J.; Sitter, A. J.; Reczek, C. M. *Biochim. Biophys. Acta* **1985**, *828*, 73.
(25) Hashimoto, S.; Tatsuno, Y.; Kitagawa, T. *Proc. Natl. Acad. Sci. U.S.A.* **1986**, *83*, 2417.

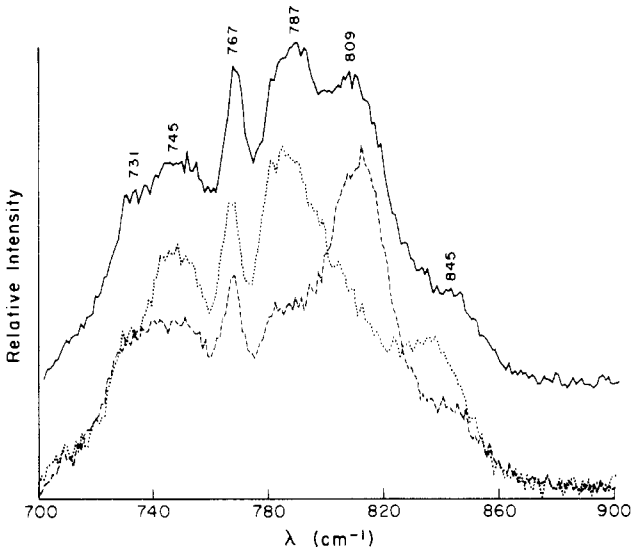


**Figure 6.** Spectral characteristics of the 812-$cm^{-1}$ band of the V–V ion in $^{16}O$ and $^{18}O$ $H_2O$ mixtures. Key: solid line, 60% $^{18}O$-enriched $H_2O$; dashed line, 100% $^{16}O$-enriched $H_2O$; dotted line, 85% $^{18}O$-enriched $H_2O$. Conditions are the same as in Figure 5, except 10 scans were averaged.

O–Ru geometries for these ions render formation of a peroxo bridge unlikely. Specifically, from the magnitude of the $^{18}O$-induced shift in $\nu_s$(Ru–O–Ru) (Table II), it is possible to calculate the dimer Ru–O–Ru bridging angles.[17] The analysis assumes that this mode is not coupled to other molecular vibrations; this assumption appears justified on the basis that bridging angles calculated for the III–III ions are 166–169°, which compare favorably with the crystallographically determined[1] angle of 165°. For the other ions listed in Table II, the calculated bridging angle varied from 154 to 180°, where the smaller angles correspond to the larger isotope shifts. On the basis of these angles, the calculated minimum intramolecular separation distance between the terminal oxo atoms ($O_t$) would be 2.7 Å when the angle is 154° or 3.7 Å at 180°. This calculation assumed that the $O_t$–Ru–Ru angle is acute and that the $O_t$–Ru–Ru–$O_t$ torsional angle is 0°. Neither of these conditions obtain for the crystalline $((bpy)_2Ru(OH_2))_2O^{4+}$ (III–III) ion, where the actual separation distance is 4.8 Å. These distances are all much larger than the oxygen–oxygen single-bond length (1.49 Å in $H_2O_2$) indicating that extreme distortion of the equilibrium structures would be required to form an intramolecular bond between the terminal oxo atoms.

Assignment of the band to the Ru=O stretching vibration of the terminal oxo atom is consistent with all of the observations. Metal–oxo stretching vibrations generally give medium-intensity RR bands whose positions are highly variable but can be found in the 800-$cm^{-1}$ region. For example, $\nu$(Mo=O) bands in structurally similar ($\mu$-oxo)molybdenum V–V dimers were found[23] at ~950 $cm^{-1}$, and $\nu(Fe^{IV}=O)$ bands have been identified[24,25] in peroxidases at ~770 $cm^{-1}$. The shift to higher energy in strong acid can be rationalized in terms of cis-bonding effects whereby protonation of the $\mu$-oxo bridging atom weakens its bonding to the ruthenium atoms allowing compensatory strengthening of other coordinate bonds.

Peroxo and ruthenyl oxo stretching modes can be discriminated experimentally by examining the band at ~50% isotopic substitution. Under these conditions, uncoupled ruthenyl oxo stretching motions in the dimer would give a band structure that was simply the summation of the separate Ru=$^{16}O$ and Ru=$^{18}O$ bands, i.e., two bands with equal intensities, one each at their characteristic frequencies, whereas for peroxo complexes a third band would be observed at an intermediate frequency corresponding to the $^{16}O$–$^{18}O$ bond in the mixed-isotope species. At 50% substitution, this band would have an intensity given by its statistical weight that is twice the intensity of the $^{16}O$–$^{16}O$ and $^{18}O$–$^{18}O$ bands. Results of such an experiment are displayed in Figure 6. The V–V ion exhibited a two-band spectrum that was very nearly the composite of spectra for the $^{16}O$-containing and $^{18}O$-containing complex ions. No new band appeared at an intermediate frequency, excluding peroxo-containing species and supporting the assignment as a $Ru^V$=O stretching mode.

**Scheme I**

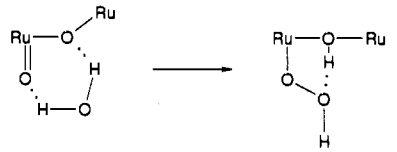

**Mechanistic Implications.** the combined data on $O_2$ isotopic distributions and aqua and oxo ligand exchange provide clear evidence for operation of two separate major pathways for water oxidation in which one or both atoms of dioxygen are derived from solvent. A minor pathway involving intramolecular oxidative elimination of terminal oxo atoms or bimolecular reaction between catalytic species in which an O–O bond is formed between a terminal oxo atom from each of the complexes[7] might exist, but its presence was not consistently detected in the various runs (Table I). For reactions involving solvent oxidation, it is necessary to explain why analogous mononuclear complexes are unable to catalyze water oxidation,[3] since there is no obvious reason why these pathways would be blocked in these ions. In the V–V ion the bridging oxo atom is relatively basic, as indicated by its protonation in strong acid. For the pathway in which O–O bond formation occurs between a terminal oxo atom and solvent, hydrogen bonding to an approaching $H_2O$ molecule could significantly enhance its nucleophilicity, hence its reactivity toward a ruthenyl ion, e.g., as in Scheme I, and might also serve an essential function in forming a hydrogen-bonding template to properly orient the solvent molecule for reaction. Alternatively, protonation of the bridging oxo atom could enhance the electrophilicity of the adjacent terminal oxo atoms, thereby promoting attack by the weakly nucleophilic water molecule. Kinetic analyses, currently in progress, will be required to assess which of these effects is the more important factor.

The pathway for which both O atoms originate in $H_2O$ is truly remarkable. Meyer has suggested[12] the possibility that intermediate species possessing bridging $O_3$ chains might form, the relatively electron-deficient central oxo atom of which is derived from solvent. Nucleophilic attack at that site by a second solvent molecule would then give an $O_2$ product containing only solvent oxygen atoms. Alternatively, diperoxo intermediates can be envisioned; e.g.

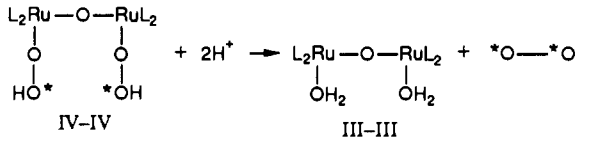


which could collapse by eliminating $H_2O_2$ or $O_2$ that contained only solvent-derived oxygen atoms. In any event, the dimer would play an essential catalytic role as reaction template, i.e., at least two ruthenium centers are necessary to form the reactive intermediates.

The importance of hydrogen bonding and protonation in conferring reactivity upon the Mn cluster within the photosystem II oxygen-evolving complex[6] is also being intensively investigated through structural modeling studies.[26-29] The various ruthenium $\mu$-oxo ions are uniquely suited to explore these relationships because they combine the properties of high catalytic activity with widely varying extents of solvent interaction, as implicit in the

(26) Stibrany, R. T.; Garum, S. M. *Angew. Chem., Int. Ed. Engl.* **1990**, *29*, 1156.
(27) Chan, M. K.; Armstrong, W. H. *J. Am. Chem. Soc.* **1990**, *112*, 4985.
(28) Bossek, U.; Weyhermüller, T.; Wieghardt, K.; Nuber, B.; Weiss, J. *J. Am. Chem. Soc.* **1990**, *112*, 6387.
(29) Micklitz, W.; Bott, S. G.; Bentsen, J. G.; Lippard, S. J. *J. Am. Chem. Soc.* **1989**, *111*, 372.

deuterium isotope shifts (Table II).

**Acknowledgment.** During the course of this study, we benefited from helpful discussions with Karl Wieghardt, C. Michael Elliott, Joann Sanders-Loehr, and Thomas M. Loehr. Dr. Loehr also generously made available to us his Raman facility. Mass spectrometric measurements were made with the technical assistance of Lorne Isabelle and Bruce Tiffany. We are grateful to these individuals, and also to the U.S. Department of Energy, Office of Basic Energy Sciences, for financial support provided under Grant DE-FG06-87ER13664.

**Registry No.** $((bpy)_2Ru(OH_2))_2O^{4+}$, 96364-19-1; $H_2O$, 7732-18-5; $Co^{3+}$, 22541-63-5.

Contribution from the Department of Chemistry and Biochemistry, University of Colorado, Boulder, Colorado 80309, Department of Organic Chemistry, University of Veszprêm, 8201 Veszprêm, Hungary, and Central Research Institute for Chemistry, Hungarian Academy of Sciences, 1525 Budapest, Hungary

# Synthesis and Characterization of (Tetramethylethylenediamine)(9,10-phenanthrenequinone)(9,10-phenanthrenediolato)copper(II), a Copper Complex Containing Mixed-Charge 9,10-Phenanthrenequinone Ligands

Gábor Speier,*[1a] Sándor Tisza,[1a] Antal Rockenbauer,[1b] Steven R. Boone,[1c] and Cortlandt G. Pierpont*[1c]

*Received May 22, 1991*

(Tetramethylethylenediamine)(9,10-phenanthrenequinone)(9,10-phenanthrenediolato)copper(II), Cu(TMEDA)(PhenCat)(PhenBQ), has been prepared by treating copper metal with a solution containing TMEDA and 9,10-phenanthrenequinone. Dark green crystals of the complex form in the monoclinic crystal system, space group $P2_1/n$, in a unit cell of dimensions $a$ = 14.331 (3) Å, $b$ = 11.079 (3) Å, $c$ = 18.471 (3) Å, $\beta$ = 101.84 (3)°, $V$ = 2870 (1) Å$^3$, and $Z$ = 4. The coordination geometry about the copper atom is square pyramidal with TMEDA and 9,10-phenanthrenediolate ligands chelated at basal sites and the 9,10-phenanthrenequinone ligand bonded at the apical position through one oxygen atom. The diolate and quinone ligands are paired together at the metal through a charge-transfer interaction. EPR spectra of the complex recorded on solid powder samples and on a single crystal show the marked anisotropy expected of a square pyramidal complex of $Cu^{2+}$. Several charge distributions are possible for the complex, but this result confirms the Cu(II)-phenanthrenediolate charge distribution in the solid state.

## Introduction

Much of the bioinorganic chemistry of catechols and related quinone molecules concerns interactions with copper. Direct coordination of the catecholate oxidation product of tyrosine to the binuclear dicopper center of tyrosinase has been proposed.[2] Elimination of the quinone as an oxidized benzoquinone restores the enzyme to its reduced form. Characterization on the amine oxidase enzymes has suggested that the pyrroloquinoline quinone (PQQ) redox cofactor interacts with a copper center of the enzyme.[3] It has not been shown that PQQ is actually a ligand, however. In one case, bovine plasma amine oxidase, the putative PQQ cofactor has been found to be a 6-hydroxydopa species (TOPA).[4] Evidence linking the copper center of the enzyme with the quinone may point to the existence of a $Cu^{II}(Cat)/Cu^{I}(SQ)$ electron-transfer step in the function of the amine oxidase enzymes.[5] Bacterial phenylalanine hydroxylase contains a reduced pterin cofactor that is directly coordinated to a Cu(II) ion.[6] The reduced pterin bears an electronic similarity to an amidophenolate species. Intramolecular electron transfer may activate the metal to the Cu(I) form necessary for molecular oxygen coordination,[7] although, no direct evidence for this has been presented. The common feature of these systems is electron transfer from the reduced catecholate to the Cu(II) center with reduction of the metal to Cu(I). This is followed by addition of molecular oxygen to the reduced metal in the course of enzymatic function.

Synthetic stoichiometric[8] and catalytic[9] catechol oxidation systems have been of interest, and many of these use molecular oxygen as an oxidant. In this context, studies have been carried out on catecholate complexes of copper. Early reports by Brown described copper(II) 3,5-di-*tert*-butylcatecholate complexes containing nitrogen-donor counterligands.[10] Structural studies on complexes of this type have shown that they may have monomeric, dimeric, or tetrameric structures.[11-13] Copper complexes of the 9,10-phenanthrenediolate ligand have been important as species which readily show catecholate oxidation to benzoquinone.[14] In

**Table I.** Crystallographic Data for Cu(TMEDA)(PhenCat)(PhenBQ)

| | | | |
|---|---|---|---|
| mol wt | 596.2 | $V$, Å$^3$ | 2870 (1) |
| color | green | $Z$ | 4 |
| cryst syst | monoclinic | $D_{calcd}$, g cm$^{-3}$ | 1.380 |
| space group | $P2_1/n$ | $D_{exptl}$, g cm$^{-3}$ | 1.38 (1) |
| $a$, Å | 14.331 (3) | $\mu$, cm$^{-1}$ | 8.0 |
| $b$, Å | 11.079 (3) | $T_{max}$, $T_{min}$ | 0.892, 0.903[a] |
| $c$, Å | 18.471 (3) | $R$, $R_w$ | 0.040, 0.049 |
| $\beta$, deg | 101.84 (3) | GOF | 1.28 |

[a] Radiation Mo K$\alpha$ (0.710 73 Å); $T$ = 294-296 K. No absorption correction was applied.

(1) (a) University of Veszprêm. (b) Hungarian Academy of Sciences. (c) University of Colorado.
(2) Winkler, M. E.; Lerch, K.; Solomon, E. I. *J. Am. Chem. Soc.* **1981**, *103*, 7001.
(3) Dooley, D. M.; Cote, C. E.; McGuirl, M. A.; Bates, J. L.; Perkins, J. B.; Moog, R. S.; Singh, I.; Knowles, P. F. In *PQQ and Quinoproteins*; Jongejan, J. A., Duine, J. A., Eds.; Kluwer: Dordrecht, The Netherlands, 1989; p 307.
(4) (a) Vellieux, F. M. D.; Huitema, F.; Groendijk, H.; Kalk, K. H.; Frank, J.; Jongejan, J. A.; Duine, J. A.; Petratos, K.; Drenth, J.; Hol, W. G. J. *EMBO J.* **1989**, *8*, 2171. (b) Janes, S. M.; Mu, D.; Wemmer, D.; Smith, A. J.; Kaur, S.; Maltby, D.; Burlingame, A. L.; Klinman, J. P. *Science* **1990**, *248*, 981.
(5) Dooley, D. M.; McIntire, W. S.; McGuirl, M. A.; Cote, C. E.; Bates, J. L. *J. Am. Chem. Soc.* **1990**, *112*, 2782.
(6) Pember, S. O.; Benkovic, S. J.; Villafranca, J. J.; Pasenkiewicz-Gierula, M.; Antholine, W. E. *Biochemistry* **1987**, *26*, 4477.
(7) Pember, S. O.; Johnson, K. A.; Villafranca, J. J.; Benkovic, S. J. *Biochemistry* **1989**, *28*, 2124.
(8) Brown, D. G.; Beckmann, L.; Ashby, C. H.; Vogel, G. C.; Reinprecht, J. T. *Tetrahedron Lett.* **1977**, 1363.
(9) (a) Speier, G. *J. Mol. Catal.* **1986**, *37*, 259. (b) Demmin, T. R.; Swerdloff, M. D.; Rogic, M. M. *J. Am. Chem. Soc.* **1981**, *103*, 5795. (c) Oishi, N.; Nishida, Y.; Ida, K.; Kida, S. *Bull. Chem. Soc. Jpn.* **1980**, *53*, 2847.
(10) Brown, D. G.; Reinprecht, J. T.; Vogel, G. C. *Inorg. Nucl. Chem. Lett.* **1976**, *12*, 399.
(11) Buchanan, R. M.; Wilson-Blumenberg, C.; Trapp, C.; Larsen, S. K.; Greene, D. L.; Pierpont, C. G. *Inorg. Chem.* **1986**, *25*, 3070.
(12) Olmstead, M. M.; Power, P. P.; Speier, G.; Tyeklar, Z. *Polyhedron* **1988**, *7*, 609.
(13) Saf'yanov, Yu. N.; Zakharov, L. N.; Struchkov, Yu. T.; Lobanov, A. V.; Cherkasov, V. K.; Abakumov, G. A. *Koord. Khim.* **1989**, *15*, 1233.
(14) Speier, G. *Inorg. Chim. Acta* **1988**, *143*, 149.

0020-1669/92/1331-1017$03.00/0 